iScience

CellPress
OPEN ACCESS

Article

Phagosomal granulocytic ROS in septic patients induce the bacterial SOS response

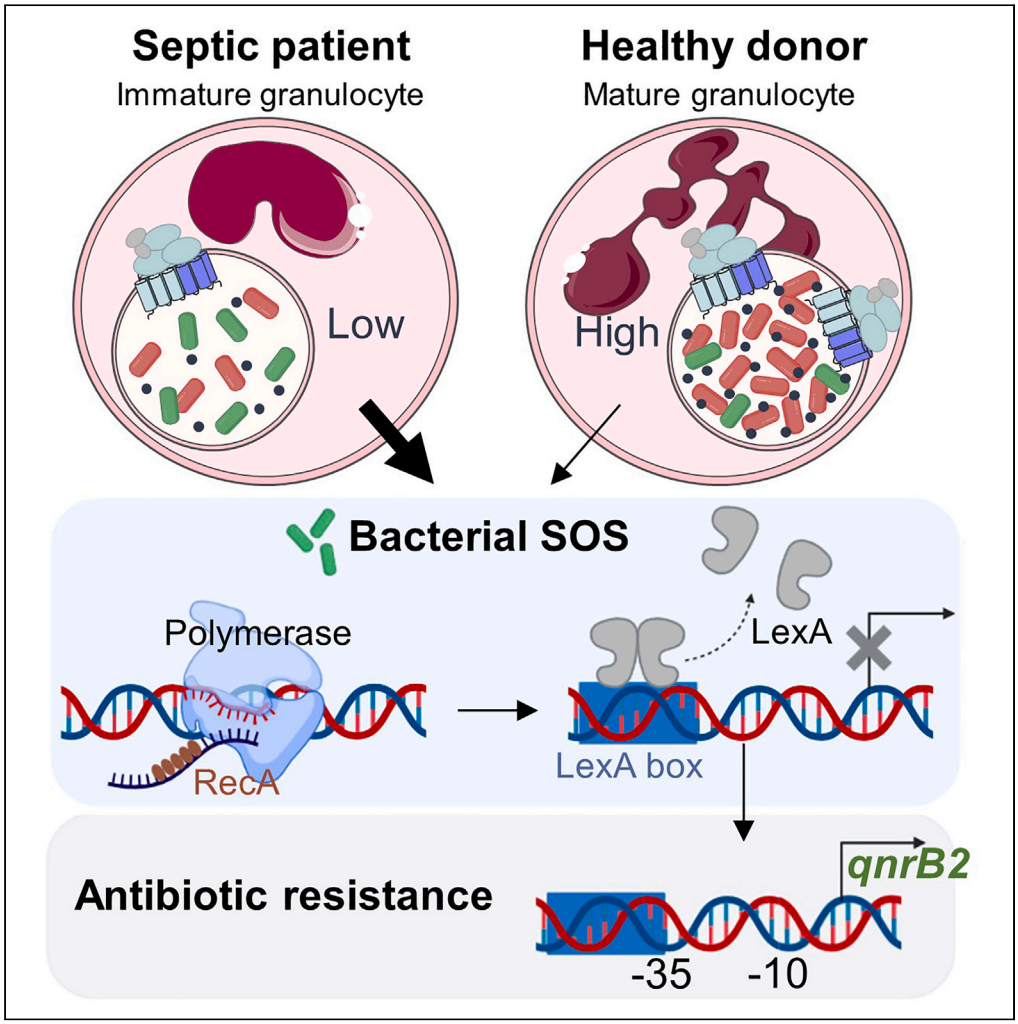

Stecy Chollet, Ana Catalina Hernandez Padilla, Thomas Daix, ..., Sandra Da Re, Robin Jeannet, Marie-Cécile Ploy

robin.jeannet@unilim.fr

Highlights

Immature granulocytes in sepsis have decreased phagocytosis and ROS production

SOS response is induced in granulocyte-phagocyted bacteria and is ROS dependent

The level of bacterial SOS induction depends on granulocyte maturation and priming

Phagocyted bacteria induce SOS-dependent quinolone resistance *qnrB2* expression

Chollet et al., iScience *27*, 109825
June 21, 2024
https://doi.org/10.1016/j.isci.2024.109825

iScience

CellPress
OPEN ACCESS

Article

Phagosomal granulocytic ROS in septic patients induce the bacterial SOS response

Stecy Chollet,[1,7] Ana Catalina Hernandez Padilla,[1,7] Thomas Daix,[1,2,3] Margaux Gaschet,[1] Bruno François,[1,2,3] Christophe Piguet,[5] Nathalie Gachard,[4,6] Sandra Da Re,[1] Robin Jeannet,[3,6,8,9,*] and Marie-Cécile Ploy[1,8]

SUMMARY

Septic patients with worst clinical prognosis have increased circulating immature granulocytes (IG), displaying limited phagocytosis and reactive oxygen species (ROS) production. Here, we developed an *ex vivo* model of incubation of human granulocytes, from septic patients or healthy donors, with *Escherichia coli*. We showed that the ROS production in Sepsis-IG is lower due to decreased activation and protein expression of the NADPH oxidase complex. We also demonstrated that the low level of ROS production and lower phagocytosis of IG in sepsis induce the bacterial SOS response, leading to the expression of the SOS-regulated quinolone resistance gene *qnrB2*. Without antimicrobial pressure, the sepsis immune response alone may promote antibiotic resistance expression.

INTRODUCTION

Mature granulocytes (MG) are the most abundant cell effectors of the innate immune response. MG specialize in pathogen recognition and phagocytosis through Fcγ receptors (CD32, CD64, CD16).[1] Phagocytosis activates reactive oxygen species (ROS) production by the NADPH oxidase complex.[1,2] Composed of 2 membrane (gp91phox and p22phox) and 3 cytoplasmic (p40phox, p67phox, and p47phox) subunits, a functional NADPH oxidase complex is necessary for bacterial clearance. Indeed, mutations in the *CYBB* (gp91phox) or *NCF1* (p47phox) genes underlie the primary immunodeficiency chronic granulomatous disease (CGD). Therefore, CGD patients have more recurrent invasive bacterial infections while their granulocytes maintain functional phagocytic activity.[3]

Sepsis, defined as a dysregulated immune response to infection, is a major cause of morbidity worldwide, affecting up to 50 million people annually, with a mortality rate reaching 20%.[4] Infection-related cytokine storm and acute MG consumption in sepsis trigger a characteristic surge in granulopoiesis that drives immature granulocyte (IG) egress from the bone marrow.[5] IG phagocytic function and ROS production are less effective than those of MG.[6,7] Increased circulating IG at arrival in the emergency department is associated with worse short-term prognosis and increased mortality in sepsis patients.[8]

Most bacteria adapt to environmental stress through the DNA damage-induced SOS response.[9] In *Escherichia coli*, more than 50 genes are part of the SOS regulon, encoding diverse functions related to DNA repair, *trans*-lesion DNA replication, and cell division arrest.[9,10] The repressor, LexA, and the activator, RecA, regulate this coordinated cellular response. LexA binds to a LexA-box sequence located in the promoter region of the regulated genes.[11]

During infection, bacteria are phagocyted by granulocytes and encounter phagosomal ROS,[1,2] which could stress bacteria via DNA damage.[12] We hypothesized that the low-level ROS production by IG early in sepsis might promote the induction of the bacterial SOS response. We report here that NADPH oxidase complex-related ROS production in granulocytes from septic patients induces the bacterial SOS response inside phagosomes. We also show that this induction of the SOS response can lead to an increased expression of the SOS-inducible quinolone resistance gene, *qnrB2*.

RESULTS AND DISCUSSION

The bacterial SOS response is induced in granulocytes' phagosomes and depends on ROS production

First, to analyze granulocyte-bacteria interactions, we developed an *ex vivo* co-culture system consisting of human granulocytes (MG from healthy donors [HD-MG] or IG from septic patients [Sepsis-IG]) and *E. coli* MG1656 derivatives (Table S1). IG are phenotypically characterized

[1]University Limoges, Inserm, CHU Limoges, RESINFIT, U 1092, F-87000 Limoges, France
[2]CHU Limoges, Service de Réanimation Polyvalente, Limoges, France
[3]Inserm CIC 1435, Limoges, France
[4]CHU Limoges, Laboratoire d'hématologie, Limoges, France
[5]CHU Limoges, Département de pédiatrie médicale, Limoges, France
[6]CNRS UMR 7276, Inserm UMR 1262, Université de Limoges, Limoges, France
[7]These authors contributed equally
[8]These authors contributed equally
[9]Lead contact
*Correspondence: robin.jeannet@unilim.fr
https://doi.org/10.1016/j.isci.2024.109825

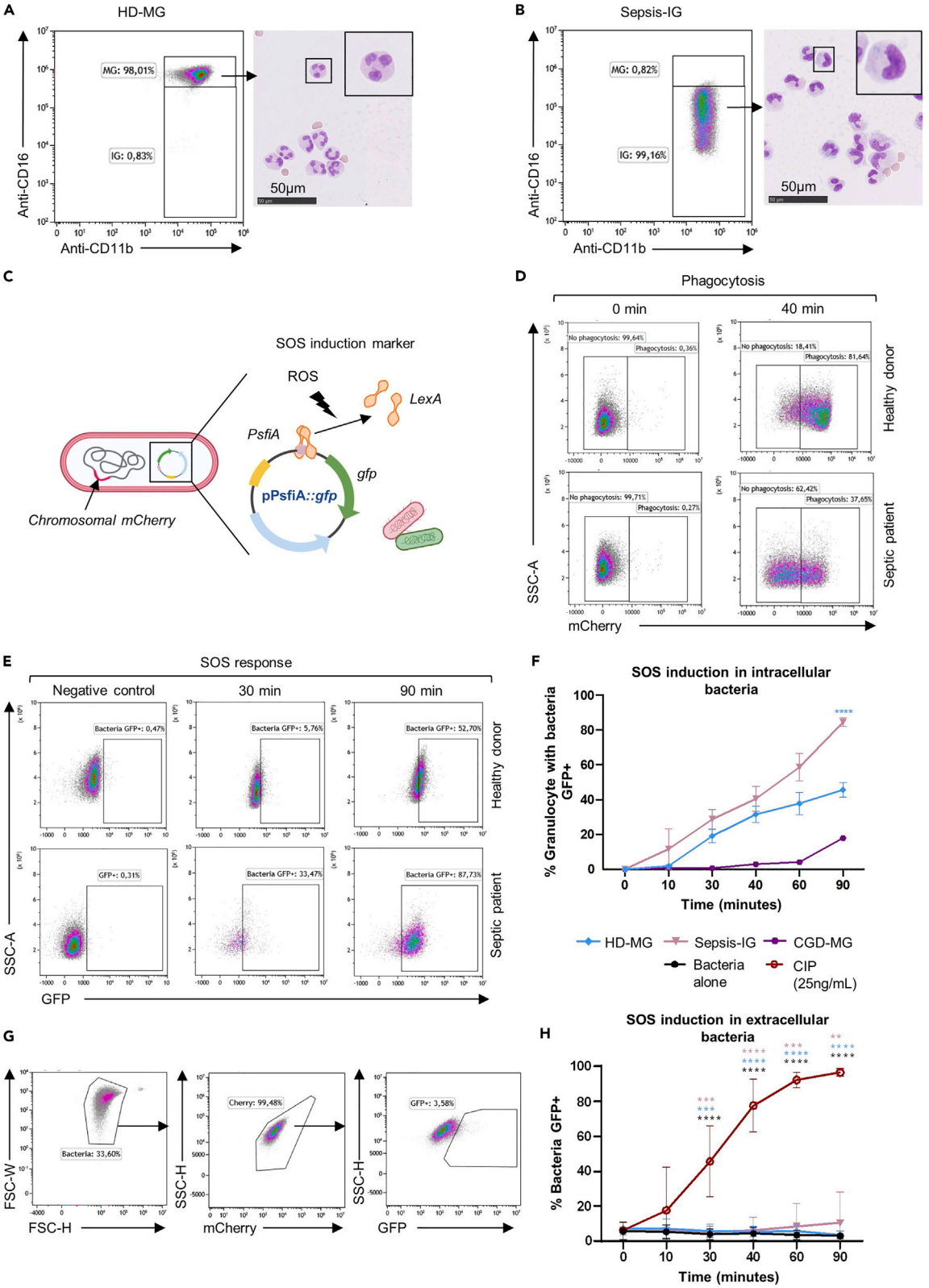
A
HD-MG
MG: 98,01%
IG: 0,83%
Anti-CD16
Anti-CD11b
50µm
B
Sepsis-IG
MG: 0,82%
IG: 99,16%
Anti-CD16
Anti-CD11b
50µm
C
SOS induction marker
ROS
LexA
PsfiA
gfp
pPsfiA::gfp
Chromosomal mCherry
D
Phagocytosis
0 min
40 min
No phagocytosis: 99,64%
Phagocytosis: 0,36%
No phagocytosis: 18,41%
Phagocytosis: 81,64%
No phagocytosis: 99,71%
Phagocytosis: 0,27%
No phagocytosis: 62,42%
Phagocytosis: 37,65%
Healthy donor
Septic patient
SSC-A
mCherry
E
SOS response
Negative control
30 min
90 min
Bacteria GFP+: 0,47%
Bacteria GFP+: 5,76%
Bacteria GFP+: 52,70%
GFP+: 0,31%
Bacteria GFP+: 33,47%
Bacteria GFP+: 87,73%
Healthy donor
Septic patient
SSC-A
GFP
F
SOS induction in intracellular bacteria
% Granulocyte with bacteria GFP+
Time (minutes)
HD-MG
Sepsis-IG
CGD-MG
Bacteria alone
CIP (25ng/mL)
G
Bacteria: 33,60%
Cherry: 99,48%
GFP+: 3,58%
FSC-W
FSC-H
SSC-H
mCherry
SSC-H
GFP
H
SOS induction in extracellular bacteria
% Bacteria GFP+
Time (minutes)

Figure 1. Characterization of mature and immature granulocytes and bacterial SOS response after phagocytosis by granulocytes

(A and B) All patient and donor samples were screened by flow cytometry to quantify the proportion of mature (MG) and immature (IG) granulocytes with the antibodies anti-CD16-PECy7 and anti-CD11b-APCCy7. Additionally, cells were stained with May-Grünwald-Giemsa for cytological characterization. (A) MGs are $CD11b^{+}$ $CD16^{high}$ and have poly-lobed nuclei, (B) while IGs are defined as $CD11b^{+}$ $CD16^{low}$ and are mainly band cells, with bean-shaped nuclei.

(C–F) MG from healthy donors (HD-MG, $n = 10$), IG from septic patients (Sepsis-IG, $n = 5$), and MG from a patient with chronic granulomatous disease (CGD-MG, $n = 1$) were incubated with mCherry-*E. coli*/pPsfiA*gfp* to assess SOS induction. (C) Plasmid system to measure SOS induction encodes the *gfp* gene under the control of the *sfiA* promoter, PsfiA, which is repressed at steady state by LexA and induced upon SOS induction. The plasmid was transformed into the mCherry-*E. coli* MG1656 with constitutive expression of chromosomal *mCherry* (red bacteria). (D, E) Representative flow cytometry density plots demonstrate (D) bacterial phagocytosis as measured by mCherry fluorescence and (E) SOS response induction measured by GFP fluorescence in mCherry+ granulocytes over time. (F) Induction of SOS response quantified as the percentage of mCherry+ (phagocytic) granulocytes exhibiting GFP fluorescence.

(G) Representative density plot of the SOS induction in extracellular bacteria by GFP expression among mCherry-*E. coli*/pPsfiA*gfp*.

(H) Induction of SOS response quantified as the percentage of extracellular GFP+ bacteria. As a control, bacteria were grown alone (black) or in the presence of ciprofloxacin at 25 ng/mL (a known SOS inductor; $n = 12$) to assess SOS induction. Microscope images (A and B) display the scale bars in the inferior left corner. Error bars represent mean ± SEM. Significance was calculated using the ANOVA test. Each star symbol represents the p value of the comparison between the curve underneath and the corresponding color curve, $^{**}p < 0.01$, $^{***}p < 0.001$, $^{****}p < 0.0001$.

by the surface expression of receptors $CD11b^{+}$, $CD62L^{high}$, $CD10^{low}$, and $CD16^{low}$ (Figures 1A and 1B).[8] To quantify bacterial SOS induction, mCherry-*E. coli* was transformed with a *gfp* expression plasmid driven by the promoter of *sfiA* (PsfiA), a gene from the SOS regulon involved in the arrest of bacterial cell division (Figure 1C). Flow cytometry analysis revealed that both HD-MG and Sepsis-IG phagocytosed mCherry-*E. coli* bacteria (Figure 1D) and induced the expression of the PsfiA*gfp* fusion (Figures 1E and 1F), suggesting an SOS response induction. Interestingly, this induction increased over time in Sepsis-IG, reaching a significantly higher level after 90 min of incubation than in HD-MG (84.5% ± 2.46% vs. 45.6% ± 4.15%, $p < 0.0001$) (Figure 1F). To assess if PsfiA*gfp* expression was induced by the ROS produced by the NADPH oxidase complex, MG from a CGD patient (CGD-MG) with a *CYBB* mutation were used as a negative control. CGD-MG did not induce PsfiA*gfp* expression (Figure 1F), indicating SOS response induction depends on NADPH complex-derived ROS. As further controls, we showed that phagocytic granulocytes from each donor type became GFP+ when incubated with the mCherry-*E. coli*/pPsfiA**gfp* strain (exhibiting constitutive *gfp* expression, Table S1), but remained GFP− when incubated with the mCherry-*E. coli*/p-*gfp* strain (lacking the *PsfiA* promoter) or with mCherry-*E. coli* MG1656 *lexA*ind3/pPsfiA*gfp* (*lexA*$^{ind-}$ mutant encoding a non-cleavable LexA protein, unable to activate the SOS response) (Figure S1; Table S1). Altogether, these results confirmed the induction we observed with the mCherry-*E. coli*/pPsfiA*gfp* strain was SOS dependent. We verified that the SOS induction was not due to using an oxidation-sensitive probe to detect ROS (Figure S2).

As granulocytes can also release ROS toward the extracellular compartment,[13,14] we assessed SOS induction in non-phagocyted extracellular bacteria (Figure 1G). The *gfp* expression in these bacteria was comparable to that of bacteria cultured without granulocytes (10.38% ± 17.65% vs. 2.93% ± 1.74%) (Figure 1H). In contrast, ciprofloxacin, a known inducer of the SOS response, strongly induced *gfp* expression, showing that the bacterial SOS response was inducible in non-phagocytosed bacteria.

IG from septic patients have decreased phagocytic activity and ROS production

Next, we quantified phagocytic capacity and ROS production in Sepsis-IG, HD-MG, and CGD-MG by flow cytometry (Figure 2A). The mCherry positivity among granulocytes reveals the proportion of phagocytic cells (Figure 2B) while mCherry mean fluorescence intensity (MFI) provides an approximate count of intracellular bacteria (Figure 2C). Sepsis-IG showed significantly lower phagocytosis capacities when compared to HD-MG and CGD-MG (Figures 2B and 2C). ROS production peaked at 30 min incubation among granulocytes performing phagocytosis and then decreased, in line with the known timing of ROS production within the early phagosome.[15] Phagocytic Sepsis-IG produced significantly less ROS than phagocytic HD-MG (7.6 times lower, $p < 0.02$) over time (Figure 2D). Surprisingly, the production of ROS in the CGD-MG was higher than in Sepsis-IG (Figure 2D). As CGD patients are unable to produce ROS with the NADPH oxidase complex,[3,16] these results likely reflect the oxidative stress induced by granulocyte metabolism.[17] Confocal microscopy imaging of bacteria incubated with granulocytes showed GFP+ mCherry-*E. coli* preferentially inside the cell (Figure 2E, white arrows) and colocalized with ROS.

Altogether, these observations indicate that (i) Sepsis-IG induce expression of the PsfiA::*gfp* SOS reporter in mCherry-*E. coli* MG1656 within the phagosome, and (ii) bacterial SOS induction is related to low ROS levels produced by the IG's NADPH oxidase complex. Indeed, the absence of phagosomal ROS leads to a lack of SOS signal (CGD-MG) (Figure 1F), while higher ROS production produces only limited SOS induction (HD-MG) (Figures 2D and 1F).

The bacterial SOS response induction is IG status and ROS dependent

Although IG are typically absent in peripheral blood, their release from the bone marrow is not exclusive to sepsis.[18] Therefore, we explored whether the bacterial SOS induction was related to the IG status or sepsis-related immune dysregulation by using IG recovered from hematopoietic stem cell donors who received granulocyte colony stimulating factor (G-CSF). G-CSF promotes the production and release of $CD34^{+}$ stem cells from the bone marrow, including IG. These G-CSF IG have not encountered pathogens or cytokines in contrast to Sepsis-IG and were considered as non-primed (Non-primed-IG). We observed that the phagocytic capacities and ROS production of Non-primed-IG and Sepsis-IG were not substantially different (Figures S3A and S3B). However, there were trends toward differences in maximum phagocytic cells, which reached only 48% at 90 min for Non-primed-IG and 77% for Sepsis-IG. Non-primed-IG showed a strong early SOS response induction that reached a plateau under 60% after 30 min (Figure S3C). This suggests that IG induce the SOS response regardless of the source. We then assess if priming with

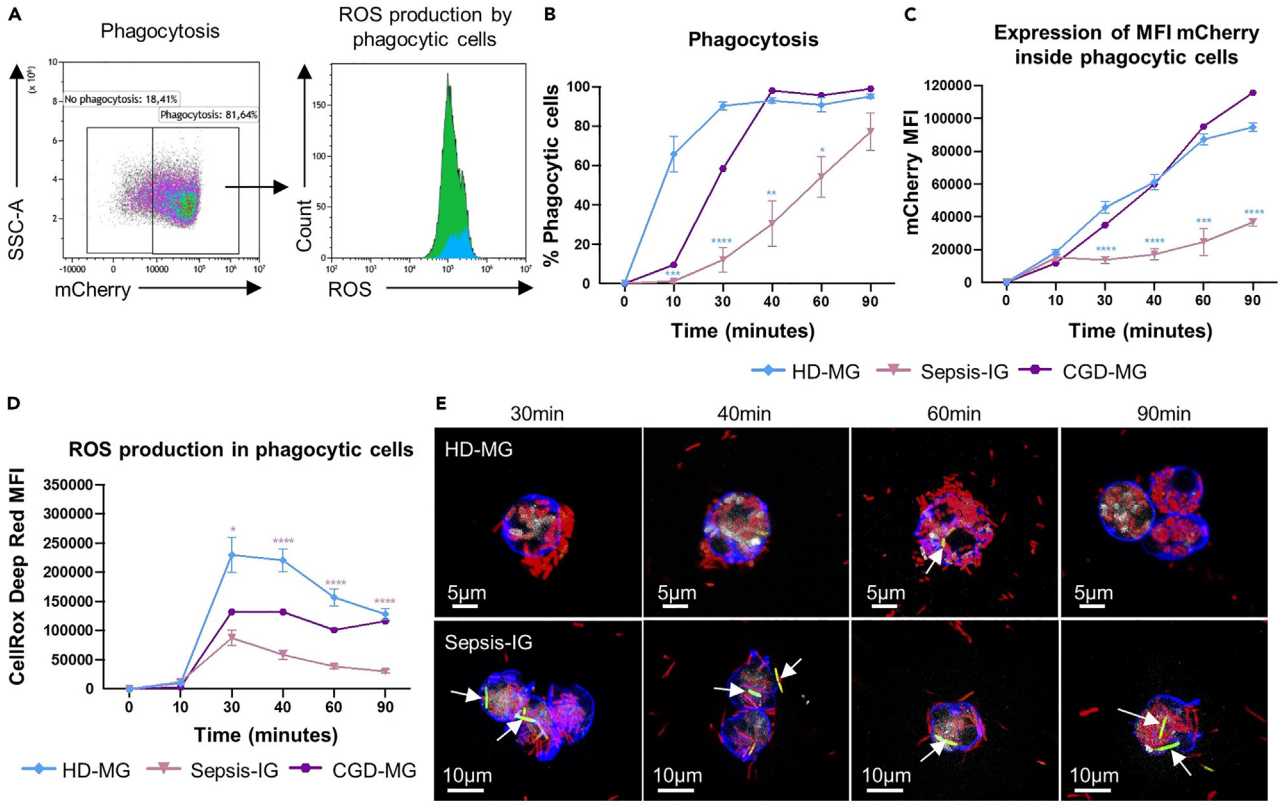

Figure 2. Granulocyte phagocytosis and ROS production

mCherry-*E. coli*/pPsfiA*gfp* were incubated with granulocytes over time and analyzed by flow cytometry (A–D) and confocal microscopy (E).

(A) Representative density plot of phagocytosis of mCherry-*E. coli* and histogram of ROS produced by phagocytic HD-MG.

(B) Percentage of granulocytes containing bacteria, (C) mCherry MFI in phagocytic cells, and (D) CellRox Deep Red MFI (reflecting ROS production), over time of bacteria co-cultured with granulocytes from HD-MG (n = 10), Sepsis-IG (n = 5), and CGD-MG (n = 1) donors.

(E) The actin filaments of granulocytes were stained with phalloidin (blue); the ROS produced by granulocytes were identified with the CellRox Deep Red probe (white). Phagocytosis of bacteria was visualized by intracellular mCherry signal (red), and SOS induction was visualized by *gfp* expression (green and white arrows). Microscope images (E) display the scale bars in the inferior left corner. Error bars represent mean ± SEM. Significance was calculated using the ANOVA test. Each color star symbol represents the p value of the comparison between the curve underneath and the corresponding color curve. *$p < 0.05$, **$p < 0.01$, ***$p < 0.001$, ****$p < 0.0001$.

soluble plasma proteins from septic patients could affect Non-primed-IG function. We found that, as expected, the priming increased phagocytosis levels to nearly the level of Sepsis-IG (around 80% phagocytic cells) (Figure S3D). However, it did not affect ROS production, suggesting that ROS production depends on the granulocyte differentiation status (Figure S3E). Interestingly, SOS induction increased in Non-primed-IG after priming (Figure S3F), suggesting that the increased SOS induction with Sepsis-IG might depend on the granulocytes' differentiation status.

Sepsis-IG exhibit decreased expression of the NADPH oxidase complex subunit and membrane receptors in line with the low phagocytosis and ROS production

We assessed the expression of two subunits of the NADPH oxidase complex, gp91phox and p47phox, by western blot after 10, 30, and 60 min of incubation with mCherry-*E. coli*. Both proteins were expressed at lower levels in Sepsis-IG vs. HD-MG (Figures 3A–3C), in line with their lower ROS production (Figure 2D). The NADPH oxidase activity depends on its expression and the assembly as an active membrane-bound complex in response to Fcγ receptor-triggered pathway stimulation (FcγR) (Figure 3G). We thus quantified the expression of these receptors by flow cytometry. We did not observe a significant difference in the expression level of CD64 (FcγRI) or CD32 (FcγRII) at baseline or after incubation with mCherry-*E. coli* (Figures 3D and 3E). However, CD16 (FcγRIII) was significantly decreased for all subsets after 10 min of incubation with bacteria (Figure 3F). Granulocyte phagocytosis induces CD16 cleavage, leading to loss of CD16 in the cell surface.[19] Moreover, CD16 is responsible for pathogen attachment, a step needed for both phagocytosis and triggering the signaling pathways required to assemble the active NADPH oxidase complex (Figure 3G).[20,21] These results suggest that the low level of CD16 in IG could explain their poor phagocytosis capacities and lower ROS production.

Altogether, our results confirm the limited antimicrobial activity of Sepsis-IG by converging mechanisms, i.e., weaker bacterial phagocytosis, and limited NADPH complex expression and activation, leading to a lower ROS production.

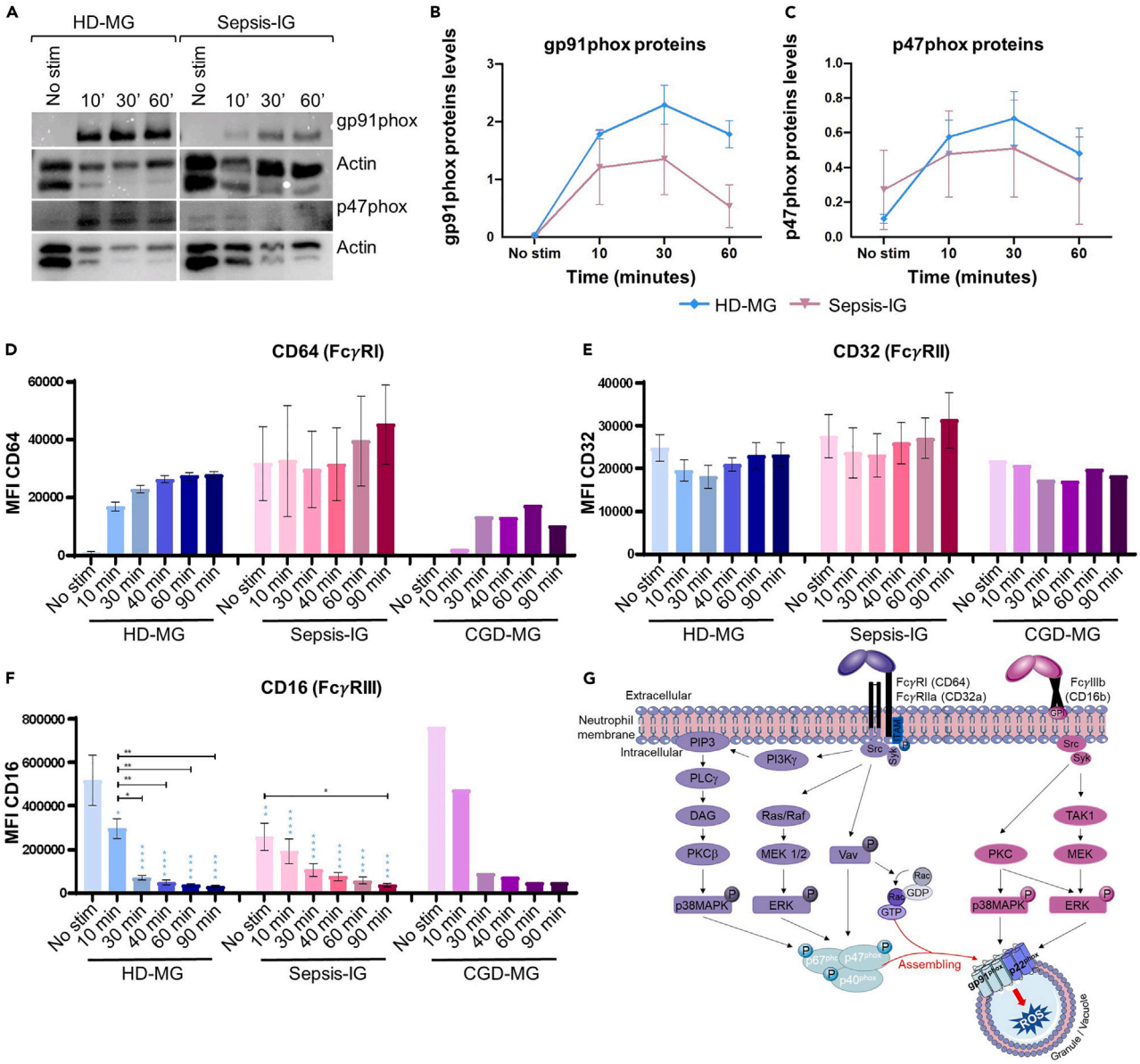

Figure 3. Expression of NADPH oxidase complex subunits and membrane receptors implicated in phagocytosis and ROS production

(A) Representative western blot (WB) of two subunits of the NADPH oxidase complex, gp91phox and p47phox, after co-culture of granulocytes with mCherry-*E. coli* over time (10, 30, 60 min).

(B and C) Relative quantification of protein expression gp91phox and p47phox from the WB results using ChemiDoc touch Imaging System and Image-lab softwares. HD-MG (n = 3) and Sepsis-IG (n = 3).

(D–F) The expression of membrane receptors implicated in phagocytosis and ROS production was analyzed by flow cytometry over time and is graphed as MFI of (D) CD64 (FcγRI), (E) CD32 (FcγRII), and (F) CD16 (FcγRIII) receptors for HD-MG (n = 6), Sepsis-IG (n = 5), and CGD-MG (n = 5).

(G) Schematic summary of the NADPH oxidase complex assembly after phosphorylation by p38MAPK and ERK1/2 through stimulated Fcγ receptors (CD64, CD32, and CD16) by pathogen recognition. Error bars represent mean ± SEM. Each bar was compared to HD-MG without bacteria (No stim) using the ANOVA test, and the p value is represented with blue stars. *$p < 0.05$, **$p < 0.01$, ***$p < 0.001$, ****$p < 0.0001$.

SOS induction in phagocyted bacteria induces the expression of the quinolone resistance gene *qnrB2*

We next explored the potential biological impact of the higher bacterial SOS induction we observed with Sepsis-IG. We used the plasmid-borne *qnrB2* gene described in a clinical *Salmonella* Keurmassar strain.[22] The *qnr* genes encoding resistance to ciprofloxacin are widespread in Enterobacterales, and the *qnrB* genes are SOS regulated.[23] HD-MG and Sepsis-IG were incubated for 90 min with the wild-type *E. coli* MG1656 strain carrying the PqnrB-*qnrB2* plasmid (Table S1). We also transformed the plasmid in the *E. coli* MG1656 *lexA*ind3 strain encoding

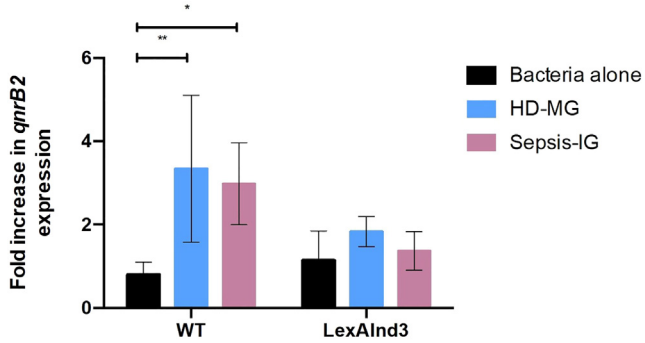

Figure 4. Expression of *qnrB2* in phagocytic HD-MG and Sepsis-IG

E. coli MG1656 (WT) or *E. coli* MG1656 *lexA*ind3 expressing a mutated non-cleavable LexA (LexAind3) carrying the pPqnrB-*qnrB2* plasmid were incubated with granulocytes. Phagocytosed bacteria were recovered after 90 min incubation with HD-MG or Sepsis-IG. Bacteria without granulocytes (Bacteria alone) were used as a control for the basal *qnrB2* expression. Results are expressed as fold-change in *qnrB2* mRNA expression. *qnrB2* transcripts were normalized to transcripts of the constitutively expressed chromosomal housekeeping gene *rpoB* and the kanamycin resistance gene, *aph(3')-IIa* gene, located on the PqnrB-*qnrB2* plasmid, under a constitutive promoter. Error bars represent mean ± SEM. ANOVA test, *$p < 0.05$, **$p < 0.01$.

a non-cleavable LexA protein. Extracellular bacteria were washed away, and granulocytes were recovered and lysed to access phagocytosed bacteria. *qnrB2* transcript copy number was quantified by quantitative reverse-transcription PCR and normalized to the copy number of the constitutively expressed chromosomal housekeeping gene *rpoB* and the plasmidic kanamycin resistance gene *aph(3')-IIa*. Incubation with HD-MG and Sepsis-IG led to a 3.34-fold ($p = 0.018$) and 2.98-fold ($p = 0.02$) increase in *qnrB2* expression, respectively, compared to bacteria incubated alone (Figure 4). This increase in transcript number is concordant with the one observed previously with an *E. coli* MG1656/pPqnrB2lexA*–*qnrB2* strain containing a mutation in the LexA-binding motif (3.6-fold increase).[23] No increase in the transcript number was observed with the *E. coli* MG1656 *lexA*ind3/pPqnrB-*qnrB2* strain, confirming that *qnrB2* expression is SOS dependent.

Although all granulocytes induced *qnrB2* expression, the biological impact would differ for all subsets. Indeed, as IG have lower bactericidal activity than MG (Figures 2B–2D), the probability of having SOS-induced viable bacteria expressing *qnrB2* in Sepsis-IG is higher than in MG in which almost all bacteria are phagocyted and non-viable.[6,16]

Antibiotic resistance has been reported in up to 26% of community-acquired sepsis,[24] and inappropriate antibiotic treatment is significantly associated with increased severity and mortality.[25] Besides *qnrB2* expression, the bacterial SOS response has been shown to potentiate antibiotic resistance through gene acquisition or increased expression[26,27] through additional mechanisms such as increased mutation rate[28] or shuffling of resistance gene cassettes via the induction of the integron integrase.[29] Furthermore, activating the SOS response can induce the dissemination of virulence genes like the cholera toxin carried by the CTX phage in *V. cholerae*, and the toxic shock syndrome toxin by *S. aureus*.[27]

Our work shows that the low ROS production level and lower IG phagocytosis in sepsis could benefit the pathogen via the SOS induction, pushing bacteria toward an adaptive response even before antimicrobial exposure. The consequences of our findings could be substantial to the patient. Indeed, our "proof of principle" study demonstrated that SOS induction by the patient's innate immune response could favor antibiotic resistance. Early analysis of the IG "profile" would help clinicians assess subpopulations of patients at risk for the emergence of antibiotic resistance.

Limitations of the study

Our study has some limitations, such as the restricted number of septic patients with high levels of circulating IG. Moreover, we limited our study to septic patients with an infection caused by gram-negative bacteria. Indeed, we explored the SOS response induced in gram-negative bacteria and used *E.coli* as a model. A patient with chronic granulomatous disease was used to confirm that the bacterial SOS response induction happens in phagosomes with functional NADPH oxidase. Patients suffering from this genetic disease are rare and rapidly treated, making them hard to enroll during the study time frame.

STAR★METHODS

Detailed methods are provided in the online version of this paper and include the following:

- KEY RESOURCES TABLE
- RESOURCE AVAILABILITY
  - Lead contact
  - Materials availability
  - Data and code availability

SUPPLEMENTAL INFORMATION

Supplemental information can be found online at https://doi.org/10.1016/j.isci.2024.109825.

ACKNOWLEDGMENTS

We thank C. Ouk and C. Carrion from the Biscem Inserm 042 CNRS 2015 for technical assistance with flow cytometry and confocal microscopy. We thank E. Pinaud, L. Tlili, and M. Sellars for their comments on the manuscript and helpful discussions.

This work was supported by the Région Nouvelle-Aquitaine and the University Hospital of Limoges. A.C.H.P. was supported by a fellowship from Fondation pour la Recherche Médicale (FRM ECO201906009178) and S.C. by a fellowship from Région Nouvelle-Aquitaine.

AUTHOR CONTRIBUTIONS

Designed experiments: S.C., A.C.H.P., R.J., and M.-C.P. Performed the experiments and data analysis: S.C. and A.C.H.P. Recruited patients and donors: T.D., B.F., C.P., and N.G. Contributed to the experiments shown in Figure 4: M.G. Helped to design the bacteria model: S.D.R. Wrote the manuscript: S.C., A.C.H.P., R.J., and M.-C.P. All authors commented on previous versions of the manuscript. Revised and edited the manuscript: R.J., S.D.R., and M.-C.P.

DECLARATION OF INTERESTS

The authors declare no competing interests.

Received: June 6, 2023
Revised: September 14, 2023
Accepted: April 24, 2024
Published: April 26, 2024

REFERENCES

1. Nordenfelt, P., and Tapper, H. (2011). Phagosome dynamics during phagocytosis by neutrophils. J. Leukoc. Biol. *90*, 271–284. https://doi.org/10.1189/jlb.0810457.
2. Piacenza, L., Trujillo, M., and Radi, R. (2019). Reactive species and pathogen antioxidant networks during phagocytosis. J. Exp. Med. *216*, 501–516. https://doi.org/10.1084/jem.20181886.
3. Arnold, D.E., and Heimall, J.R. (2017). A Review of Chronic Granulomatous Disease. Adv. Ther. *34*, 2543–2557. https://doi.org/10.1007/s12325-017-0636-2.
4. Rudd, K.E., Johnson, S.C., Agesa, K.M., Shackelford, K.A., Tsoi, D., Kievlan, D.R., Colombara, D.V., Ikuta, K.S., Kissoon, N., Finfer, S., et al. (2020). Global, regional, and national sepsis incidence and mortality, 1990–2017: analysis for the Global Burden of Disease Study. Lancet *395*, 200–211. https://doi.org/10.1016/S0140-6736(19)32989-7.
5. Manz, M.G., and Boettcher, S. (2014). Emergency granulopoiesis. Nat. Rev. Immunol. *14*, 302–314. https://doi.org/10.1038/nri3660.
6. Drifte, G., Dunn-Siegrist, I., Tissières, P., and Pugin, J. (2013). Innate Immune Functions of Immature Neutrophils in Patients With Sepsis and Severe Systemic Inflammatory Response Syndrome. Crit. Care Med. *41*, 820–832. https://doi.org/10.1097/CCM.0b013e318274647d.
7. Taneja, R., Sharma, A.P., Hallett, M.B., Findlay, G.P., and Morris, M.R. (2008). IMMATURE CIRCULATING NEUTROPHILS IN SEPSIS HAVE IMPAIRED PHAGOCYTOSIS AND CALCIUM SIGNALING. Shock *30*, 618–622. https://doi.org/10.1097/SHK.0b013e318173ef9c.
8. Daix, T., Guerin, E., Tavernier, E., Mercier, E., Gissot, V., Hérault, O., Mira, J.-P., Dumas, F., Chapuis, N., Guitton, C., et al. (2018). Multicentric Standardized Flow Cytometry Routine Assessment of Patients With Sepsis to Predict Clinical Worsening. Chest *154*,

617–627. https://doi.org/10.1016/j.chest.2018.03.058.

9. Erill, I., Campoy, S., and Barbé, J. (2007). Aeons of distress: an evolutionary perspective on the bacterial SOS response. FEMS Microbiol. Rev. *31*, 637–656. https://doi.org/10.1111/j.1574-6976.2007.00082.x.
10. Courcelle, J., Khodursky, A., Peter, B., Brown, P.O., and Hanawalt, P.C. (2001). Comparative Gene Expression Profiles Following UV Exposure in Wild-Type and SOS-Deficient *Escherichia coli*. Genetics *158*, 41–64. https://doi.org/10.1093/genetics/158.1.41.
11. Fernández de Henestrosa, A.R., Ogi, T., Aoyagi, S., Chafin, D., Hayes, J.J., Ohmori, H., and Woodgate, R. (2002). Identification of additional genes belonging to the LexA regulon in Escherichia coli: Novel LexA-regulated genes in E. coli. Mol. Microbiol. *35*, 1560–1572. https://doi.org/10.1046/j.1365-2958.2000.01826.x.
12. Dwyer, D.J., Kohanski, M.A., Hayete, B., and Collins, J.J. (2007). Gyrase inhibitors induce an oxidative damage cellular death pathway in *Escherichia coli*. Mol. Syst. Biol. *3*, 91. https://doi.org/10.1038/msb4100135.
13. Winterbourn, C.C., Kettle, A.J., and Hampton, M.B. (2016). Reactive Oxygen Species and Neutrophil Function. Annu. Rev. Biochem. *85*, 765–792. https://doi.org/10.1146/annurev-biochem-060815-014442.
14. Warnatsch, A., Tsourouktsoglou, T.-D., Branzk, N., Wang, Q., Reincke, S., Herbst, S., Gutierrez, M., and Papayannopoulos, V. (2017). Reactive Oxygen Species Localization Programs Inflammation to Clear Microbes of Different Size. Immunity *46*, 421–432. https://doi.org/10.1016/j.immuni.2017.02.013.
15. Valenta, H., Erard, M., Dupré-Crochet, S., and Nüβe, O. (2020). Molecular and Cellular Biology of Phagocytosis, *1246*, pp. 153–177.
16. Leliefeld, P.H.C., Wessels, C.M., Leenen, L.P.H., Koenderman, L., and Pillay, J. (2016). The role of neutrophils in immune dysfunction during severe inflammation. Crit. Care *20*, 73. https://doi.org/10.1186/s13054-016-1250-4.
17. Curi, R., Levada-Pires, A.C., Silva, E.B.d., Poma, S.d.O., Zambonatto, R.F., Domenech, P., Almeida, M.M.d., Gritte, R.B., Souza-Siqueira, T., Gorjão, R., et al. (2020). The Critical Role of Cell Metabolism for Essential Neutrophil Functions. Cell. Physiol. Biochem. *54*, 629–647.
18. Ui Mhaonaigh, A., Coughlan, A.M., Dwivedi, A., Hartnett, J., Cabral, J., Moran, B., Brennan, K., Doyle, S.L., Hughes, K., Lucey, R., et al. (2019). Low Density Granulocytes in ANCA Vasculitis Are Heterogenous and Hypo-Responsive to Anti-Myeloperoxidase Antibodies. Front. Immunol. *10*, 2603. https://doi.org/10.3389/fimmu.2019.02603.
19. Wang, Y., Wu, J., Newton, R., Bahaie, N.S., Long, C., and Walcheck, B. (2013). ADAM17 cleaves CD16b (FcγRIIIB) in human neutrophils. Biochim. Biophys. Acta Mol. Cell Res. *1833*, 680–685.
20. Alemán, O.R., Mora, N., and Rosales, C. (2021). The Antibody Receptor Fc Gamma Receptor IIIb Induces Calcium Entry via Transient Receptor Potential Melastatin 2 in Human Neutrophils. Front. Immunol. *12*, 657393. https://doi.org/10.3389/fimmu.2021.657393.
21. Belambri, S.A., Rolas, L., Raad, H., Hurtado-Nedelec, M., Dang, P.M.-C., and El-Benna, J. (2018). NADPH oxidase activation in neutrophils: Role of the phosphorylation of its subunits. Eur. J. Clin. Invest. *48*, e12951. https://doi.org/10.1111/eci.12951.
22. Garnier, F., Raked, N., Gassama, A., Denis, F., and Ploy, M.-C. (2006). Genetic Environment of Quinolone Resistance Gene *qnrB2* in a Complex *sul1* -Type Integron in the Newly Described *Salmonella enterica* Serovar Keurmassar. Antimicrob. Agents Chemother. *50*, 3200–3202. https://doi.org/10.1128/AAC.00293-06.
23. Da Re, S., Garnier, F., Guérin, E., Campoy, S., Denis, F., and Ploy, M.C. (2009). The SOS response promotes *qnrB* quinolone-resistance determinant expression. EMBO Rep. *10*, 929–933. https://doi.org/10.1038/embor.2009.99.
24. Rhee, C., and Klompas, M. (2020). Sepsis trends: increasing incidence and decreasing mortality, or changing denominator? J. Thorac. Dis. *12*, S89–S100. https://doi.org/10.21037/jtd.2019.12.51.
25. Murray, C.J., Ikuta, K.S., Sharara, F., Swetschinski, L., Robles Aguilar, G., Gray, A., Han, C., Bisignano, C., Rao, P., Wool, E., et al. (2022). Global burden of bacterial antimicrobial resistance in 2019: a systematic analysis. Lancet *399*, 629–655. https://doi.org/10.1016/S0140-6736(21)02724-0.
26. Baharoglu, Z., and Mazel, D. (2014). SOS, the formidable strategy of bacteria against aggressions. FEMS Microbiol. Rev. *38*, 1126–1145. https://doi.org/10.1111/1574-6976.12077.
27. Fornelos, N., Browning, D.F., and Butala, M. (2016). The Use and Abuse of LexA by Mobile Genetic Elements. Trends Microbiol. *24*, 391–401. https://doi.org/10.1016/j.tim.2016.02.009.
28. Crane, J.K., Alvarado, C.L., and Sutton, M.D. (2021). Role of the SOS Response in the Generation of Antibiotic Resistance *In Vivo*. Antimicrob. Agents Chemother. *65*, e00013-21. https://doi.org/10.1128/AAC.00013-21.
29. Guerin, É., Cambray, G., Sanchez-Alberola, N., Campoy, S., Erill, I., Da Re, S., Gonzalez-Zorn, B., Barbé, J., Ploy, M.-C., and Mazel, D. (2009). The SOS Response Controls Integron Recombination. Science *324*, 1034. https://doi.org/10.1126/science.1172914.
30. Tlili, L., Ploy, M.-C., and Da Re, S. (2021). Microniches in biofilm depth are hot-spots for antibiotic resistance acquisition in response to *in situ* stress. Preprint at Microbiology *1*. https://doi.org/10.1101/2021.11.03.467100.
31. Datsenko, K.A., and Wanner, B.L. (2000). One-step inactivation of chromosomal genes in *Escherichia coli* K-12 using PCR products. Proc. Natl. Acad. Sci. USA *97*, 6640–6645. https://doi.org/10.1073/pnas.120163297.
32. Drevets, D.A., Canono, B.P., and Campbell, P.A. (2015). Measurement of Bacterial Ingestion and Killing by Macrophages. Curr. Protoc. Immunol. *109*, 14.6.1–14.6.17. https://doi.org/10.1002/0471142735.im1406s109.

STAR★METHODS

KEY RESOURCES TABLE

REAGENT or RESOURCE	SOURCE	IDENTIFIER
Antibodies		
AmCyan Mouse Anti-Human CD45 (2D1)	BD Biosciences	Cat#339192; RRID:AB_647361
FITC Anti-Human Lineage Cocktail 2 (lin2) (CD3, CD14, CD19, CD20, CD56)	BD Biosciences	Cat# 643397; RRID:AB_1645743
APC-Cy™7 Mouse Anti-Human CD11b (ICRF44)	BD Biosciences	Cat# 557754; RRID:AB_396860
PE-Cy™7 Mouse Anti-Human CD16 (3G8)	BD Biosciences	Cat# 557744; RRID:AB_396850
BUV661 Mouse Anti-Human CD32 (FLI8.26)	BD Biosciences	Cat#741611; RRID:AB_2871019
Brillant Violet 650™ Anti-Human CD15 (SSEA-1) (W6D3)	Biolegend	Cat#323034; RRID:AB_2563840
Brillant Violet 605™ Anti-Human CD64 (10.1)	Biolegend	Cat# 305034; RRID:AB_2566237
NOX2/gp91^{phox} Polyclonal Antibody	Thermofisher	Cat# bs-3889R
p47^{phox} Antibody	Cellsignaling	Cat#4312
Goat Anti-Rabbit IgG (H + L)-HRP	BIO-RAD	Cat#1706515
Bacterial and virus strains		
For strains used in this study see Table S1	see Table S1	see Table S1
Biological samples		
Peripheral blood sample from septic, chronic granulomatous disease patients and healthy donors	University Hospital Center of Limoges (CHU of Limoges, France)	N/A
Peripheral blood sample from hematopoietic stem cell donors	Center for biological resources of the CHU of Limoges, France	N/A
Chemicals, peptides, and recombinant proteins		
EasySep Direct Human Neutrophil Isolation kit	STEMCELL TECHNOLOGIES	Cat#19666
May-Grünwald dyes	CellaVision	Cat#320070
Giemsa dyes	CellaVision	Cat#320310
ViaKrome 808 Fixable Viability Dye	Beckman coulter	Cat#C36628
DAPI solution 1 mg/mL	BD Biosciences	Cat#564907
CytoPainter Phalloidin-iFluor 405 Reagent	Abcam	Cat#ab176752
Reactive Oxygen Species (ROS) Detection Assay Kit	Abcam	Cat#ab287839
RNeasy Mini Kit	Qiagen	Cat#74104
Turbo-DNA free kit	Thermofischer	Cat#AM1907
PrimeScript RT Reagent Kit (Perfect Real Time)	Takarabio	Cat#RR037B
Experimental models: Organisms/strains		
For plasmids used in this study see Table S1	see Table S1	see Table S1
Oligonucleotides		
For primers and probes used in this study see Table S1	see Table S1	see Table S1
Software and algorithms		
NDP view software	Hamamatsu	N/A
Kaluza 2.1 software	Beckman	N/A
IMARIS 9.6 software	Bitplane	N/A
Image-lab software v6.0	BIO-RAD	N/A
Prism 8.4.3 software	Graphpad	N/A

RESOURCE AVAILABILITY

Lead contact

Further information and reagent requests may be directed to the lead contact, Robin Jeannet (robin.jeannet@unilim.fr).

Materials availability

This study did not generate new unique reagents.

Data and code availability

All data reported in this paper will be made available by the lead contact upon request.

No original code is reported in this paper.

Any additional information required to re-analyze the data reported in this paper is available from the lead contact on request.

EXPERIMENTAL MODEL AND STUDY PARTICIPANT DETAILS

Septic patients, chronic granulomatous disease (CGD) patient and healthy donors

Peripheral blood (PB) samples from all patients and donors were collected at the University Hospital Center of Limoges (CHU of Limoges), France, in accordance with the ethical principles of the Declaration of Helsinki and with the approval of the local ethical committee (CPP number: 18.11.30.42116; Clinicaltrial.gov: NCT03846596). Blood samples from septic patients were collected only if the patient filled the following criteria: having a diagnosis of sepsis within the last 24 h, being admitted to the ICU, and having >80% of the granulocyte population consisting of IG in peripheral blood as quantified by flow cytometry (Figures 1A and 1B) after labeling the cells with Fixable Viability dye, CD45, Lin2, CD15, CD11b and CD16 antibodies.

For non-primed IGs, IGs were collected from hematopoietic stem cell donors during the course of Granulocyte-colony stimulating factor (G-CSF) treatment for stem cell mobilization, with donor consent (Number CODECOH AC-2021-4790) in the Center for biological resources of the CHU of Limoges.

E. coli strains and plasmids

Bacterial strains and plasmids used in this study are summarized in Table S1.

Construction of the mCherry-*E. coli* MG1656 lexAind3 strain

The mCherry-*E. coli* MG1656 *lexA*ind3 strain was constructed by transduction of a P1 lysate carrying the *km-frt-mcherry* cassette[30] at the λatt of an *E. coli* MG1656 *lexA*ind3 receiver strain. The kanamycin resistance gene was deleted by FLP recombinase, as previously described.[31] Colonies were screened by Sanger sequencing for the *mCherry* gene (primers lATT-ext5 and lATT-ext3, Table S1). *mCherry* expression was verified by flow cytometry.

Construction of the *p-gfp* plasmid

The *p-gfp* plasmid was constructed by deleting the PsfiA* sequence from the p*PsfiA*gfp* plasmid using the In-Fusion HD cloning kit (Clontech) and DelPsfiARev and DelPsfiAFwd primers (Table S1). Deletion was confirmed by Sanger sequencing using the primers Km-verif-3 and MRVD-2 (Table S1), and by the loss of GFP fluorescence as assessed by flow cytometry.

Bacterial culture

Strains were grown overnight at 37°C under agitation at 300 rpm in Luria-Bertani (LB) medium supplemented with kanamycin (25 μg/mL) when required. A 1:100 dilution was incubated under the same conditions until it reached an OD_{600} of 0.6–0.8. The measured OD_{600} was used to calculate the volume required for a final concentration of 5×10^8 bacteria/mL (OD_{600} of 1) for incubation with granulocytes.

METHOD DETAILS

Isolation of granulocytes

IG and Mature granulocytes (MG) were obtained by negative magnetic sorting from PB using the EasySep Direct Human Neutrophil Isolation kit (STEMCELL). 5 mL of PB was incubated for 5 min at room temperature with an isolation cocktail and RapidSphere from the kit according to the manufacturer's instruction. Phosphate buffered saline (PBS) (Eurobio Scientific) was added to a final volume of 12 mL, and the tube was placed in the "The Big Easy" magnet (STEMCELL) for 10 min, before pouring the granulocyte containing supernatant into a new tube. The process was repeated twice to achieve high purity of the granulocytic population. A lower cutoff of granulocytes (IG or MG) concentration was set at 90% among total cells collected as quantified by flow cytometry. Isolated granulocytes were counted using a Countess 3FL Automated cell Counter (Invitrogen).

Priming of non-primed-IG

The granulocytes from stem cells donors were incubated in plasma from septic patients at a concentration of 10 × 10^6 cells/mL for 10 min at 37°C. Granulocytes were then washed once with PBS and resuspended in RPMI 1640 medium (Eurobio).

Morphology analysis of IG

After isolation, the granulocytes were resuspended in RPMI 1640 medium at a concentration of 1 x 10^6 cells/mL. 100 µL was centrifuged over a microscope slide using the Epredia cytocentrifuge Cytospin 4 (Thermofischer) and slides were stained with May-Grünwald-Giemsa dyes (CellaVision) before image acquisition with a NanoZoomer RS2 (Hamamatsu) and analysis with NDP view software (Hamamatsu).

Granulocyte-bacteria co-culture

The isolated granulocytes were incubated with mCherry-*E. coli* strains (Table S1) at a ratio of 200 bacteria per 1 granulocyte, at 37°C in a water bath. Incubation was performed in hemolysis tubes in RPMI 1640 medium, supplemented with 10% heat-inactivated fetal bovine serum (Eurobio), 1% non-essential amino acids (Gibco), L-glutamine (200 mM, Gibco), sodium pyruvate solution (100 mM, Gibco) and MEM vitamins solution (100X, Gibco). Samples from shorter timepoints were maintained on ice until processing.

Clearance of extracellular bacteria

To recover phagocyted bacteria, samples were placed on ice prior to density gradient centrifugation at 300 × *g* for 8 min at 4°C using ice-cold 50% sucrose.[32] After discarding the upper phase (containing extracellular bacteria), the sucrose phase was diluted with an equal volume of cold PBS and centrifuged at 250 × *g* for 5 min to pellet granulocytes.

Cytometry analyses

Immunophenotyping, phagocytosis, ROS production and SOS induction measurements described below were acquired with a CytoFLEX LX (Beckman coulter) and analyzed using Kaluza 2.1 software (Beckman). For immunophenotyping the granulocytes were staining with Fixable Viability dye, CD45, Lin2, CD15, CD11b, CD16, CD32 and CD64 antibodies.

Phagocytosis measurement

After incubating granulocytes with mCherry-*E. coli* strains (Table S1), half of each sample was taken for flow cytometry and confocal microscopy analysis, respectively. For flow cytometry, granulocytes were stained with the viability marker DAPI and fixed with a 2% formaldehyde solution (Merck) in PBS. For confocal microscopy, granulocytes were fixed and permeabilized using 4% formaldehyde solution (Merck) for 10 min at 4°C. After washing, samples were stained with CytoPainter Phalloidin-iFluor 405 Reagent (Abcam) for 30 min at 4°C. After a further wash with PBS, the pellet was resuspended with 25 µL of PBS and deposited on a microscope slide (SUPERFROST PLUS, Thermofisher). Confocal images were acquired with a LSM880 (Zeiss) and analyzed using IMARIS 9.6 software (Bitplane).

Reactive oxygen species (ROS) measurement

After incubation with mCherry-*E. coli* (for 10, 30, 60 min), granulocyte ROS was detected using the Reactive Oxygen Species Detection Assay Kit (CellRox Deep Red, Abcam) as described in the supplier protocol. In brief, 1µL of the oxidation-sensitive probe was added to 0.25 million cells in 200 µL and incubated for 30 min at 37°C in a water bath. Cells were processed for flow analysis as above.

Assessment of bacterial SOS response induction

Induction of SOS response was analyzed by flow cytometry and confocal microscopy. For flow cytometry, the fixed granulocytes incubated with bacteria were acquired (CytoFLEX LX, Beckman coulter) and analyzed for GFP expression. A parallel condition incubating mCherry-*E. coli* with granulocytes was performed by adding culture media instead of the oxidation-sensitive probe to make sure the SOS induction results were replicable to those with the probe, independently from the presence of the oxidation-sensitive probe.

For confocal microscopy, after incubation with Reactive Oxygen Species Detection Assay Kit, the granulocytes incubated with mCherry-*E. coli*/pPsfiA*gfp* were centrifuged 5 min at 200 × *g* and permeabilized with a solution of 4% formaldehyde (Merck) for 10 min at 4°C. After incubation, the samples were stained with CytoPainter Phalloidin-iFluor 405 Reagent (Abcam) for 30 min at 4°C in the dark to stain granulocytes' actin filaments. After washing with PBS, the pellet was resuspended with 25 µL of PBS and deposited on a microscope slide (SUPERFROST PLUS, Thermofisher). Pictures were acquired by confocal microscopy (LSM880 Zeiss) and analyzed using IMARIS 9.6 software (Bitplane).

Quantification of *qnrB2* transcripts

Sample preparation

E. coli MG1656/pPqnrB-*qnrB2* and *E. coli* MG1656 *lex*Aind3/pPqnrB-*qnrB2* were incubated either alone or at a 200:1 ratio with granulocytes from healthy donors (n = 5), stem cells donors (n = 5), or septic patients (n = 4) for 90 min at 37°C in a water bath. Granulocytes and extracellular bacteria were separated as described above.

RNA extraction

The cellular pellet was resuspended in 1 mL ice-cold sterile water and incubated for 10 min on ice. Then, a 15 min incubation with RNase A at room temperature (Macherey-Nagel) was performed to eliminate contaminating eukaryotic RNA. RNase A was removed by centrifugation (>12000 × *g* for 10 min, RT), and the pellet was washed in filtered PBS. The final product was immediately processed with the RNeasy Mini Kit (Qiagen), following the manufacturer's instructions for recovery of bacterial RNA. Contaminating DNA was removed from RNA samples using the Turbo-DNAfree kit (ThermoFisher Scientific). Purified RNA was quantified using a Nanodrop ND1000 spectrophotometer (Thermo Fisher Scientific).

Quantitative reverse transcription-polymerase chain reaction (RT-qPCR)

Reverse-transcription (RT) was performed using the PrimeScript RT Reagent Kit (Perfect Real Time, Takara), in a final volume of 60 μL. RNA concentrations were all adjusted to a final quantity equivalent to that of the least concentrated sample; a matching negative control of without RT enzyme mix was prepared in parallel for each sample. cDNA were quantified with the Perfecta fastmix II (QuantaBio), following manufacturer's instructions with appropriate primers (10 μM) and a FAM-probe (10 μM) (Table S1). Samples were processed in technical triplicates. A standard curve was done using a range of 10^8 to 10^2 copies of a plasmid containing the targeted genes. Each gene (chromosomal *rpoB* and plasmid *qnrB2* and *aph(3')-IIa*) was targeted separately. The chromosomal housekeeping *rpoB* gene was used for normalization. To account for the multiple plasmid copies per bacteria, the plasmid gene conferring constitutive expression of kanamycin resistance (*aph(3')-IIa*) was used for normalization of the *qnrB2* expression.

Western blot

Granulocytes were incubated with mCherry-*E. coli* for 10, 30 and 60 min at 37°C in a water bath, the tubes were centrifuged for 5 min at 300 × *g*. The granulocyte pellets were lysed with RIPA lysis buffer (Santa Cruz) supplemented with a protease (PMSF 200 mM, Santa Cruz) and phosphatase inhibitor (Na-Orthovandate 100 nM, Santa Cruz) for 30 min in ice, centrifuged for 20 min at 18000 × *g* and the supernatant containing proteins was kept. Protein concentration was estimated from standard range of BSA (2 mg/mL, BIO-RAD) using Bradford's reagent (BIO-RAD) and a Multiskan FC at 595 nm (Thermofisher).

Proteins (30 μg/μL) were denatured for 5 min at 95°C with 4X Laemmli buffer (BIORAD) supplemented with 10% β-mercaptoethanol (BIORD), and separated by SDS-PAGE before transferring to a PolyVinyliDene Fluoride (PVDF) transfer membrane (Life Sciences). Membranes were blocked using 5% BSA (Bovine Serum Albumin) (Euromedex) in Trisma Base 10X (TBS, Sigma) supplemented with 0.1% Tween 20 solution (Sigma) for 1 h at room temperature and incubated with primary antibodies: anti-gp91phox (Thermofisher) and anti-p47phox (Cell-signaling) at a dilution of 1:1000 in 5% BSA in TBS-Tween20 overnight at 4°C. The primary antibodies were detected with HRP-conjugated secondary antibody anti-rabbit (BIORAD) at a dilution of 1:5000 in 5% skin milk (Millipore) in TBS-Tween20 for 1 h at RT. β-actin polymerase Antibody (Invitrogen) was used as a control at a dilution of 1:2000 with 5% skin milk in TBS-Tween20 for 1 h at RT and was detected via anti-rabbit secondary antibody (BIORAD) at a dilution of 1:5000 in 5% skin milk for 1 h at RT. A chemiluminescent HRP substrate was used for signal detection (Millipore) on a ChemiDoc touch Imaging System (BIO-RAD). Densitometric quantification was performed using Image-lab software v6.0 (BIO-RAD).

Statistical analysis

All graphs were created using Graphpad prism 8.4.3 software. The geometric mean (MFI of mCherry, CD64, CD32, CD16, and ROS production (CellRox deep red), % phagocytic cells, % bacteria GFP+ production and SOS induction) of each variable measured by flow cytometry was compared between each condition and the results of incubation between mCherry-*E. coli* and HD-MG at the matching time-point using the two-way ANOVA test. Statistical significance was defined as a $p < 0.05$, and significant *p*-values represented for each point as follows: $*p < 0.05$, $**p < 0.01$, $***p < 0.001$, $****p < 0.0001$.